

Commentary: Carbon Nanotubes, CdSe Nanocrystals, and Electron–Electron Interaction

Louis Brus

Chemistry Department, Columbia University, New York, New York 10027

ABSTRACT To celebrate the tenth anniversary of *Nano Letters*, this short commentary discusses a scientific issue of current interest, increased electron–electron interactions in nanostructures. The two major factors of reduced dimensionality and low screening are analyzed. Carbon nanotubes and graphene are molecular in many of their properties and show strong electron–electron interactions. In specific circumstances, excited-state decay by exciton generation rather than phonon generation can be efficient in carbon nanotubes.

KEYWORDS Carbon nanotubes, CdSe nanocrystals, electron–electron interaction

Nano Letters has become a significant journal in the 10 years of its existence. Founding Editor Paul Alivisatos deserves our gratitude for his initial vision, hard work, and steadfast guidance. The journal has thrived because of high standards and a broad perspective, incorporating relevant areas of physics, materials science, engineering, as well as chemistry. Indeed, nanoscience is inherently interdisciplinary. Nanoscience thrives in academic chemistry departments because chemistry students have a broad range of synthetic and physical interests. Modern chemistry is diverse and inclusive.

The past decade has seen the rise of carbon nanoscience—a field which combines organic chemistry and solid-state physics. Many significant carbon nanotube and graphene papers have appeared in *Nano Letters*. The nanoelectronics of aromatic carbon π and π^* electrons involves strong and well-understood chemical bonding. The fusing of these bonding ideas with solid-state spatial periodicity leads to remarkable physical properties. I now discuss electron–electron interaction, including “excitons”, in single-wall carbon nanotubes (SWNTs), comparing them with other organic conjugated polymers and with inorganic CdSe nanocrystals. There have been several good recent reviews in this general area.^{1–3}

Hydrogenic excitons are bound electron–hole pairs attracted to each other by their Coulomb interaction. They undergo correlated relative motion and lie in energy below the free carrier dissociation limit (i.e., band gap). In bulk 3D CdSe (high frequency dielectric constant $\epsilon = 8.2$), the Coulomb interaction is strongly screened, and the carrier effective masses are low. As a consequence, the exciton is bound by only 15 meV, in comparison with the

In molecular orbital language, strong electron–electron interaction corresponds to excited electronic states involving extensive configuration interaction.

1.84 eV band gap. Excitons thermally dissociate into free carriers at room temperature.

Electron–electron interaction increases in nanostructures (and in molecules) compared with bulk semiconductors, and thus excitons become more strongly bound. There are two independent factors: dimensionality and dielectric screening. Twenty years ago when GaAs/GaAlAs quantum wells were first explored, Schmitt-Rink, Chemla, and Miller thoroughly analyzed the electronic states.⁴ They pointed out the critical importance of dimensionality, in situations where screening does not change because the local environment has the same dielectric constant as the nanostructure itself. If one confines the exciton to a 2D plane in a 3D semiconductor, the exciton binding energy and Coulomb interaction go up by a factor of 4 compared with the 3D exciton. This increase simply comes from analysis of screened Coulomb and kinetic energies in 2D versus 3D. Furthermore, if the electron and hole are mathematically confined to a 1D line, the Coulomb energy actually diverges. The distinction between free and bound electron hole states disappears.

This analysis points toward the importance of thin nano-wire geometry for high electron–electron interaction.

Zero-dimensional CdSe nanocrystals of 4 nm diameter show quantum confinement. The electron and hole are confined by the nanocrystal walls and have strongly increased overlap. Yet, because of this strong individual confinement, their relative motion is not strongly correlated, unlike the case in Coulomb bound 3D bulk excitons. In nanocrystals the net Coulomb interaction does increase with respect to the bulk exciton. However, relatively little of the electric field between electron and hole fringes out of compact nanocrystals, and thus dielectric screening is similar to that in bulk CdSe. The net Coulomb interaction is about 0.1 eV, a small fraction of the nanocrystal band gap. This Coulomb energy is less than the electron and hole kinetic energies. In a normal hydrogenic correlated exciton, the Coulomb energy is twice as large as the kinetic energies. In a sense, it is a misnomer to call this confined electron–hole state an “exciton”.

The situation is very different in 1–2 nm diameter semiconducting SWNTs. In SWNTs excitons are bound by their mutual Coulomb attraction, show correlated motion, and can dissociate into free carriers along the tube length. Ando first predicted very strong electron–electron interactions in SWNT, producing deeply bound excitons and significant band gap renormalization.⁵ Exciton binding energies were experimentally measured by a comparison of two-photon and one-photon luminescence excitation spectra.^{6,7} In the (6,5) SWNT the exciton binding energy in Figure 1 is about 0.43 eV.⁶ This implies an exciton Coulomb interaction on the order of 0.8 eV, assuming a normal correlated exciton structure where the net binding energy is half the Coulomb energy. In this tube the (renormalized) band gap is only 1.7 eV, so the exciton Coulomb energy is half the band gap—quite remarkable! This (6,5) tube has a diameter of 0.8 nm, and the exciton extends for about 2.4 nm along the length as shown. Thus the electronic geometry is approaching 1D.

SWNT impact ionization experiments also indicate extremely strong electron–electron interaction. Intense exciton luminescence is generated by “hot” accelerated electrons in single SWNTs.⁸ Excitons are created as the hot electron relaxes to the conduction band edge. This process competes with decay by phonon generation (i.e., heat production), which is the normal relaxation route for hot carriers in bulk semiconductors. Perebeinos and Avouris⁹ theoretically calculated the threshold rate of exciton generation to be 10^{15} s^{-1} . It only takes 1 fs for an electron with sufficient excess kinetic energy to generate an exciton! The lifetime broadening of the initial hot electron state would be on the order of 1 eV. This rate is so fast that it almost does not make sense to consider hot single electrons as well-defined quantum states in SWNTs.

This rate is many orders of magnitude faster than impact exciton generation in bulk semiconductors. Both re-

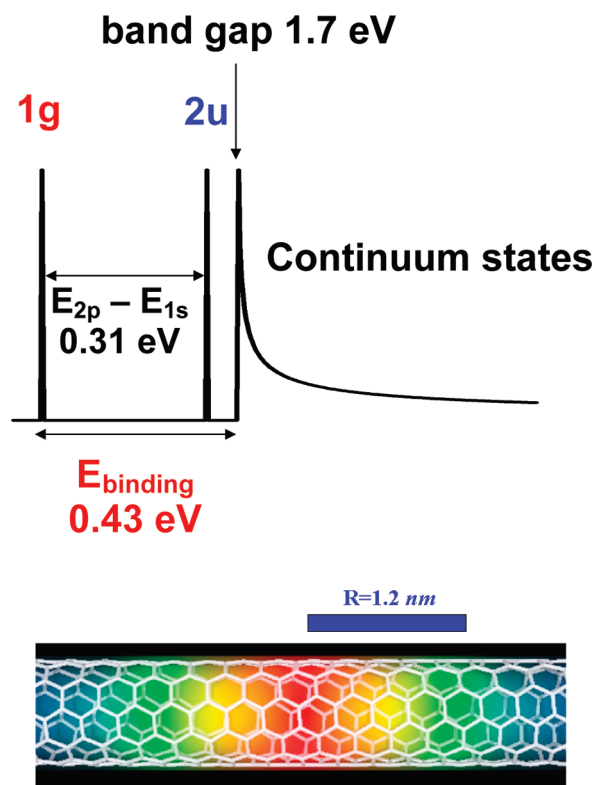


FIGURE 1. (top) Schematic diagram of exciton bound states, nano-tube band gap, and continuum optical absorption in a (6,5) SWNT. (bottom) Calculated spatial extent along the tube length of the lowest 1s bound exciton state. This figure is adapted from ref 6.

duced dimensionality and low dielectric screening contribute to this fast rate. The experimental SWNT exciton structure implies that the electron–hole Coulomb interaction is screened by a $\epsilon = 3.3$ effective dielectric constant.⁹ This is about a factor of 3 smaller than that in CdSe.

A recent important SWNT discovery reports photovoltaic current multiplication for high photon excitation energy, in the presence of a longitudinal electric field.¹⁰ This result also implies very strong electron–electron interaction, although a detailed mechanism is lacking. Optically excited, high-energy single excitons far above the band gap produce two or three pairs of separated electrons and holes. The initially excited state decays by exciton (bound or ionized) generation, assisted by the electric field, rather than by phonon generation. This is analogous to the impact ionization experiment discussed above.

Other near 1D conjugated organic polymers, such as poly(*p*-phenylenevinylene) (PPV), also show strong electron correlation and electron–hole interaction.^{11,12} In comparison with these species, SWNTs have the great advantage of being structurally rigid with very rare structural defects. Rigidity in SWNTs creates high mobility for free carriers and excitons, with the concomitant weak Franck–Condon coupling of these species to nanotube vibrations. In SWNTs there is no self-trapping of free carriers or optical excited states. SWNTs are solid-state-like

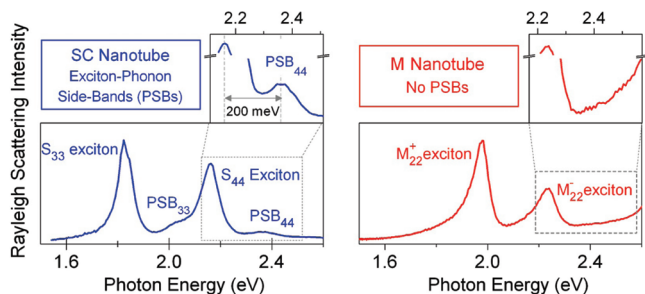


FIGURE 2. Excited electronic states of individual semiconductor (left side) and metallic (right side) SWNTs. PSB refers to a vibronic sideband (in the LO phonon) associated with each main exciton origin electronic transition in semiconductor tubes. The spectra are measured using resonant Rayleigh scattering. This figure adapted from ref 13.

in the sense that high mobility exists along the tube. Yet SWNTs are molecular-like in that the optical absorption spectrum looks like a molecular spectrum,¹³ with intense, discrete transitions to neutral, deeply bound excited electronic states in Figure 2. The dominance of discrete optical transitions over residual continuum absorption is a direct consequence of strong electron–electron interaction¹⁴ and even occurs in metallic SWNTs.

Both graphene and SWNTs offer low dimensionality and low screening.

The electrons are on the surface, and their electric fields extend out of the structures. Physical properties are sensitive to the local environment—a typical molecular attribute. A fractional quantum Hall liquid is observed in 2D graphene, suspended in vacuum at low temperature.^{15,16} This state is a classic signature of strong

electron correlation. The data imply an electron–electron effective dielectric constant ϵ about 1.¹⁵ Graphene in vacuum is a 2D system that essentially shows no screening! SWNTs are near 1D systems with effective screening near $\epsilon = 3$, at least for exciton purposes. In SWNTs efficient exciton generation processes exist that are not well understood. In the next 10 years, *Nano Letters* will surely report new experiments that both deepen our understanding of this new electron–electron physics and teach us how to use exciton generation phenomena for efficient solar energy utilization.

Acknowledgment. I have enjoyed informative discussions with Mark Hybertsen, Eran Rabani, Philip Kim, Tony Heinz, and David Reichman. Our effort in this area is supported by the DOE Basic Energy Sciences EFRC program under DE-SC0001085. I thank S. Berciaud for Figure 2.

REFERENCES AND NOTES

- (1) Prezzi, D.; Molinari, E. *Phys. Status Solidi* **2006**, *203*, 3602–3610.
- (2) Scholes, G.; Rumbles, G. *Nat. Mater.* **2006**, *5*, 683–696.
- (3) Avouris, Ph.; Freitag, M.; Perebeinos, V. *Nat. Photonics* **2008**, *2*, 341–350.
- (4) Schmitt-Rink, S.; Chemla, D. S.; Miller, D. A. B. *Adv. Phys.* **1989**, *38*, 89–188.
- (5) Ando, T. *J. Phys. Soc. Jpn.* **1997**, *66*, 1066–1073.
- (6) Wang, F.; Dukovic, G.; Brus, L.; Heinz, T. *Science* **2005**, *308*, 838–841.
- (7) Maulzsch, J.; Pomraenke, R.; Reich, S.; Chang, E.; Prezzi, D.; Ruini, A.; Molinari, E.; Strano, M.; Thomsen, C.; Lienau, C. *Phys. Rev. B* **2005**, *72*, 241402R.
- (8) Chen, J.; Perebeinos, V.; Freitag, M.; Tsang, J.; Fu, Q.; Liu, J.; Avouris, Ph. *Science* **2005**, *310*, 1171–1173.
- (9) Perebeinos, V.; Avouris, Ph. *Phys. Rev. B* **2006**, *74*, 121410R.
- (10) Gabor, N.; Zhong, Z.; Bosnick, K.; Park, J.; McEuen, P. *Science* **2009**, *325*, 1367–1370.
- (11) Bredas, J.-L.; Cornil, J.; Beljonne, D.; Dos Santos, D.; Shuai, Z. *Acc. Chem. Res.* **1999**, *32*, 267–276.
- (12) Kirova, N. *Polym. Int.* **2008**, *57*, 678–688.
- (13) Berciaud, S.; Voisin, C.; Yan, H.; Chandra, B.; Caldwell, R.; Shan, Y.; Brus, L.; Hone, J.; Heinz, T. *Phys. Rev. B*, in press.
- (14) Spataru, C.; Ismail-Beigi, S.; Benedict, L.; Louie, S. *Phys. Rev. Lett.* **2004**, *92*, 196401.
- (15) Bolotin, K.; Ghahari, F.; Shulman, M.; Stormer, H.; Kim, P. *Nature* **2009**, *462*, 196–199.
- (16) Du, X.; Skachko, I.; Duerr, F.; Luican, A.; Andrei, E. Y. *Nature* **2009**, *462*, 192–195.